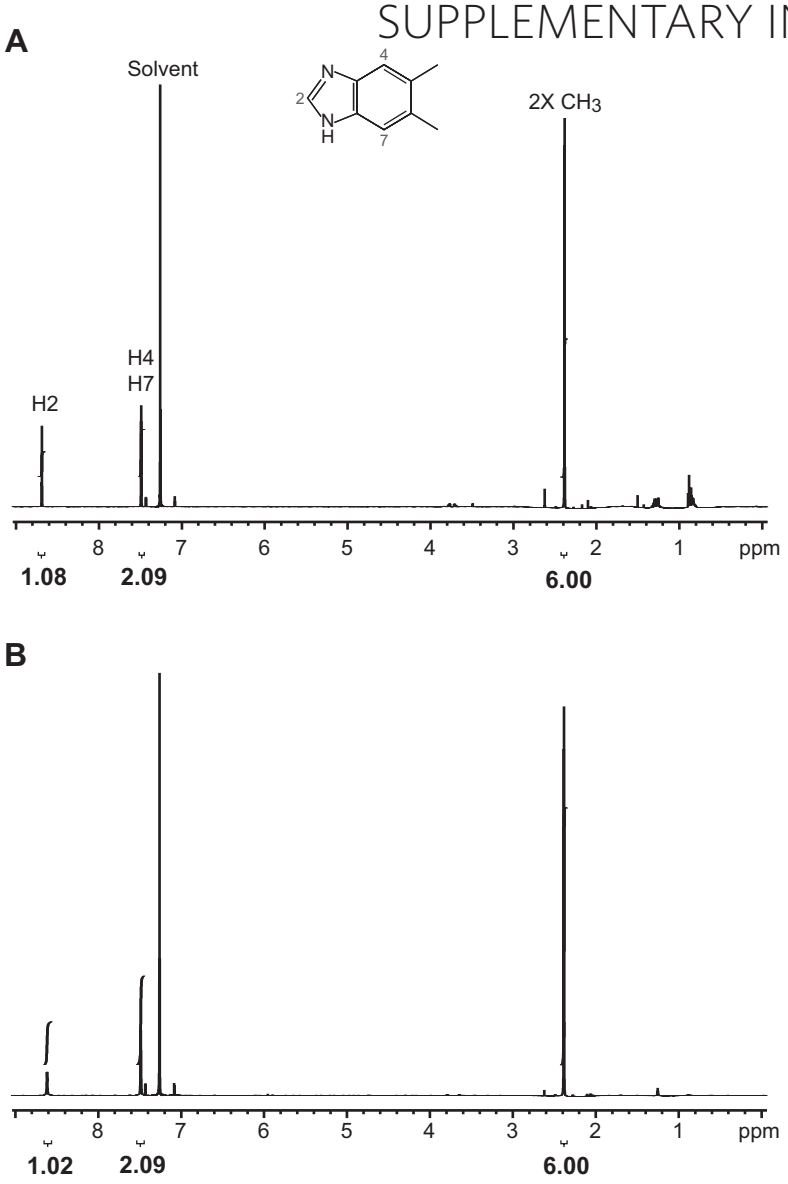

Supplementary Figure 1. ^{1}H NMR analysis shows that the BluB reaction product is DMB. Reactions containing 25 µmol FMN, 875 µmol NADPH, 1.4 µmol BluB, and 0.13 µmol SsuE were incubated for 6 h and quenched by addition of 6.4% trichloroacetic acid. The mixtures were concentrated and DMB purified by preparative HPLC with a C18 column [0.1% trifluoroacetic acid in water, 20-30% linear gradient of methanol over 30 min,10 ml min^{-1}]. An authentic standard of DMB (Sigma) was prepared similarly. ^{1}H NMR spectra of **(A)** DMB produced by the BluB-catalyzed reaction, and **(B)** an authentic standard of DMB in $CDCl_3$, recorded on a Varian 600 MHz Fourier Transform NMR spectrometer, are shown with peaks corresponding to the indicated protons in DMB. Numbers in bold indicate integral values. The peaks at 8.6 and 7.5 ppm are restored to the previously observed positions, 8.0 and 7.4 ppm[1], following pH neutralization (not shown). Identities were further confirmed by mass spectrometry (ES^+: m/z = 147, $[M+H]^+$) and UV/vis (λ_{max} = 205, 276, and 284).

[1] Maggio-Hall, L. A., Dorrestein, P. C., Escalante-Semerena, J. C. & Begley, T. P. Formation of the dimethylbenzimidazole ligand of coenzyme B(12) under physiological conditions by a facile oxidative cascade. Org Lett 5, 2211-3. (2003).

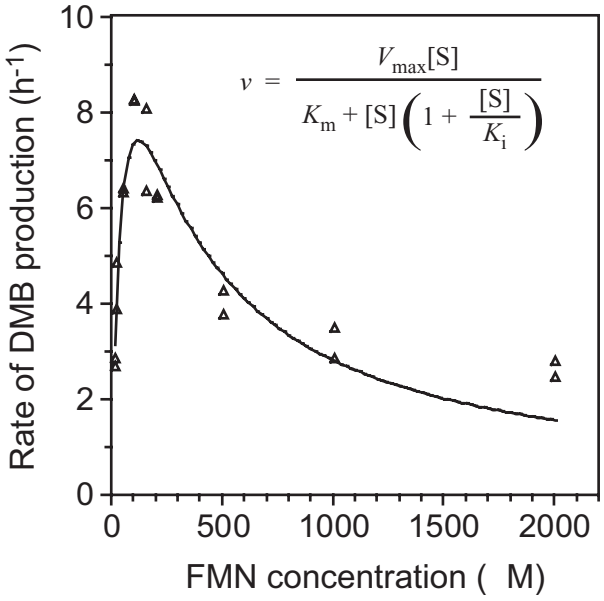

Supplementary Figure 2. Inhibition of BluB by FMN. Initial rates of DMB formation measured at various concentrations of FMN were fit to a curve given by the equation shown using KaleidaGraph (Synergy Software).

Supplementary Table 1. Initial rate of FMN reduction is not enhanced by BluB.

	FMN Reduction Rate ($\mu M\ min^{-1}$)[a]	
	NADH	NADPH
No Enzyme	3.8 ± 0.2	4.9 ± 1.7[b]
BluB	3.7 ± 0.2	6.0 ± 0.5[b]
SsuE	7.1 ± 0.5	370 ± 22[c]

[a] Reactions contained 100 μM FMN, 40 mM NADH or NADPH, and 1 μM enzyme in a final volume of 100 μl. A_{450} measurements were recorded every 9 sec on a SPECTRAmax Plus 384 plate reader (Molecular Devices). FMN reduction, measured as the rate of decrease in $A_{450}\ min^{-1}$, was converted to μM FMN using the extinction coefficient for FMN at 450 nm, 12.2 $mM^{-1}\ cm^{-1}$. The average of 4 independent reactions with standard deviation is presented. A background rate of 0.3 $\mu M\ min^{-1}$ was subtracted to obtain the final values.

[b] These values represent an average of 8 reactions.

[c] These reactions contained 10-fold less SsuE, and therefore the rate was adjusted by multiplying by 10.

Supplementary Table 2. Initial rate of BluB-catalyzed DMB synthesis is enhanced in the presence of SsuE.

	Rate of DMB formation (h^{-1})[a]	
	5 mM NADPH	20 mM NADPH
BluB	2.8 ± 1.6	19 ± 7
SsuE	No Activity	No Activity
BluB + SsuE	47 ± 6	41 ± 10

[a] The initial rate of DMB formation in reactions containing 100 μM FMN, 5 or 20 mM NADPH, and 10 μM BluB and/or 1 μM SsuE are reported. Values represent the average and standard deviation of three independent experiments.

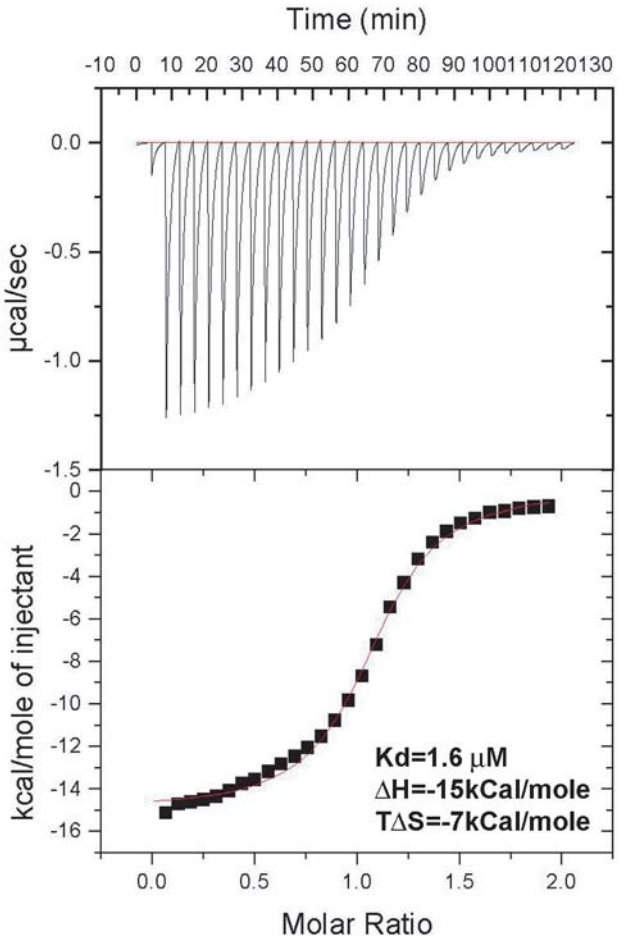

Supplementary Figure 3. Determination of K_d of BluB for FMN by isothermal titration calorimetry. FMN was titrated into apo-BluB. Isothermal titration calorimetry was conducted with a Microcal MCS ITC at 23º C. Approximately 2 mL of the BluB solution was loaded into the sample cell, while FMN was loaded into the injection syringe. Subsequently, 25 injections of 10 L FMN were added to the sample cell to give a final injectant to sample cell molar ratio ~2:1. Sufficient time was allowed between injections for the heat generated to re-equilibrate. Titration data were fit to a single binding site model32 using Origin ITC software (V. 5.0, Microcal Software Inc.). The heat of complex formation for each injection is shown in the top panel, and the data have been modeled to a single binding site per monomer in the lower panel.

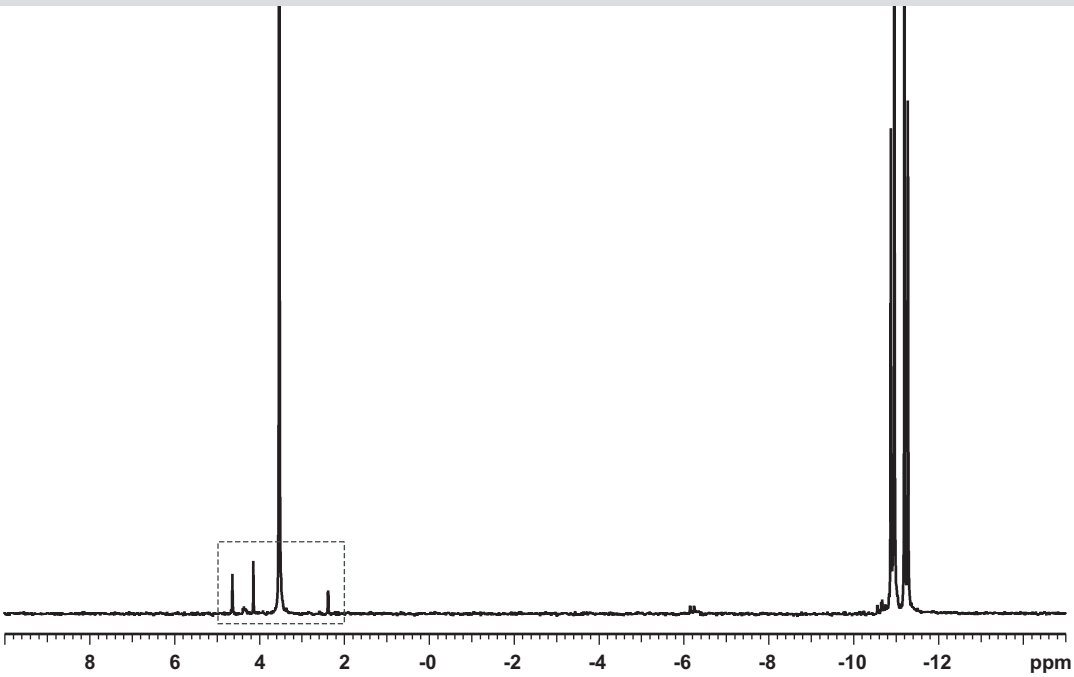

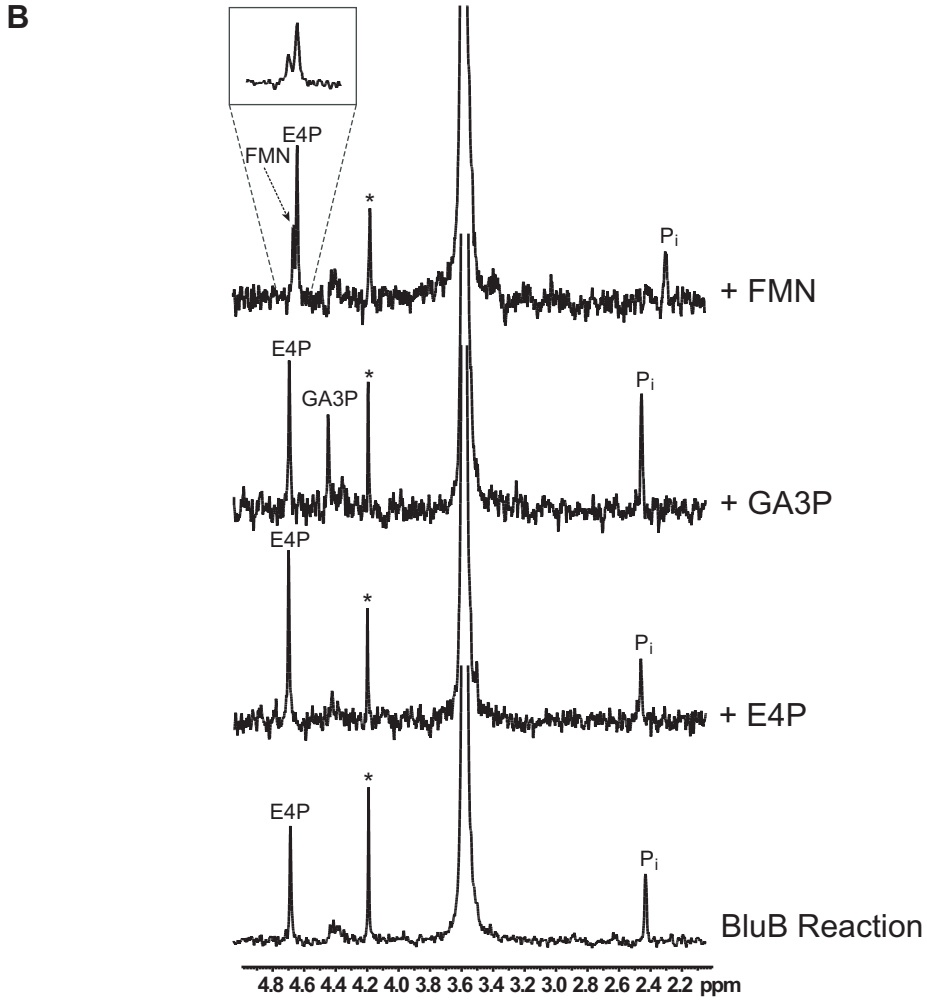

Supplementary Figure 4. ^{31}P NMR analysis shows that the BluB reaction mixture contains E4P. The $^{31}P\{^{1}H\}$ NMR spectrum (260 MHz) of the BluB reaction mixture, quenched by passage through a 30,000 MWCO filter (Microcon), concentrated, and dissolved in 10% D_2O in water, is shown in **A**. The large peaks at -11.2, -10.8, and 3.5 ppm correspond to $NADP^+$. Spectra of the boxed region in A, alone and spiked with 125 M E4P, GA3P, or FMN, are shown in **B**. The peaks marked E4P, GA3P, P_i, and FMN correspond to authentic standards, and * represents an unknown species present in the reaction. An expansion of the peaks corresponding to E4P and FMN is shown in the inset.

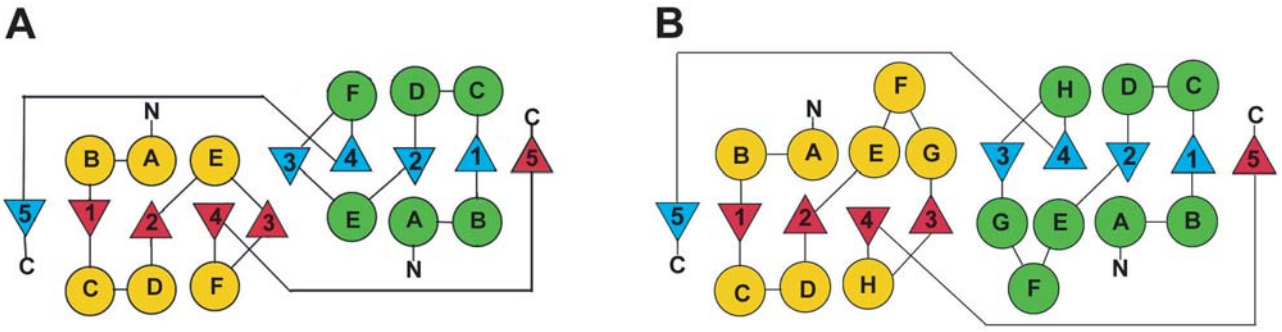

Supplementary Figure 5. Topology diagrams. Topology diagrams corresponding to BluB **(A)** and *E. coli* nitroreductase NfsA **(B)** are shown. Helices are represented as circles and β-strands as triangles. The orientation of the triangle indicates either antiparallel or parallel strands. Other oxido/nitro reductases structurally similar to BluB have additional helical insertions after 2. Helices C and D are longer in BluB, forming the lid domain.

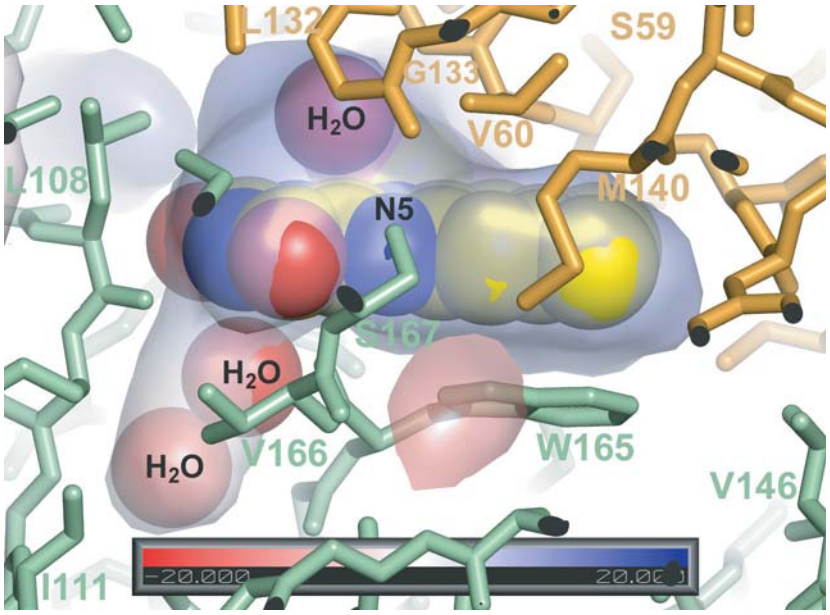

Supplementary Figure 6. Space filling model of flavin and surrounding waters. The molecular surface was calculated in the absence of flavin. The surface is colored according to electrostatic potential and rendered semi-transparent to reveal flavin within. The N5 atom on flavin has been labeled as a point of reference. Flavin is carefully confined within the binding pocket excluding alternative substrates. Surrounding protein residues that define this binding pocket are rendered as sticks. A conformational change in the flavin would necessarily result in a structural rearrangement, due to the close confinement. This rearrangement accounts for the crystal disintegration that was observed when reduced crystals were back-soaked in an oxygenated buffer.

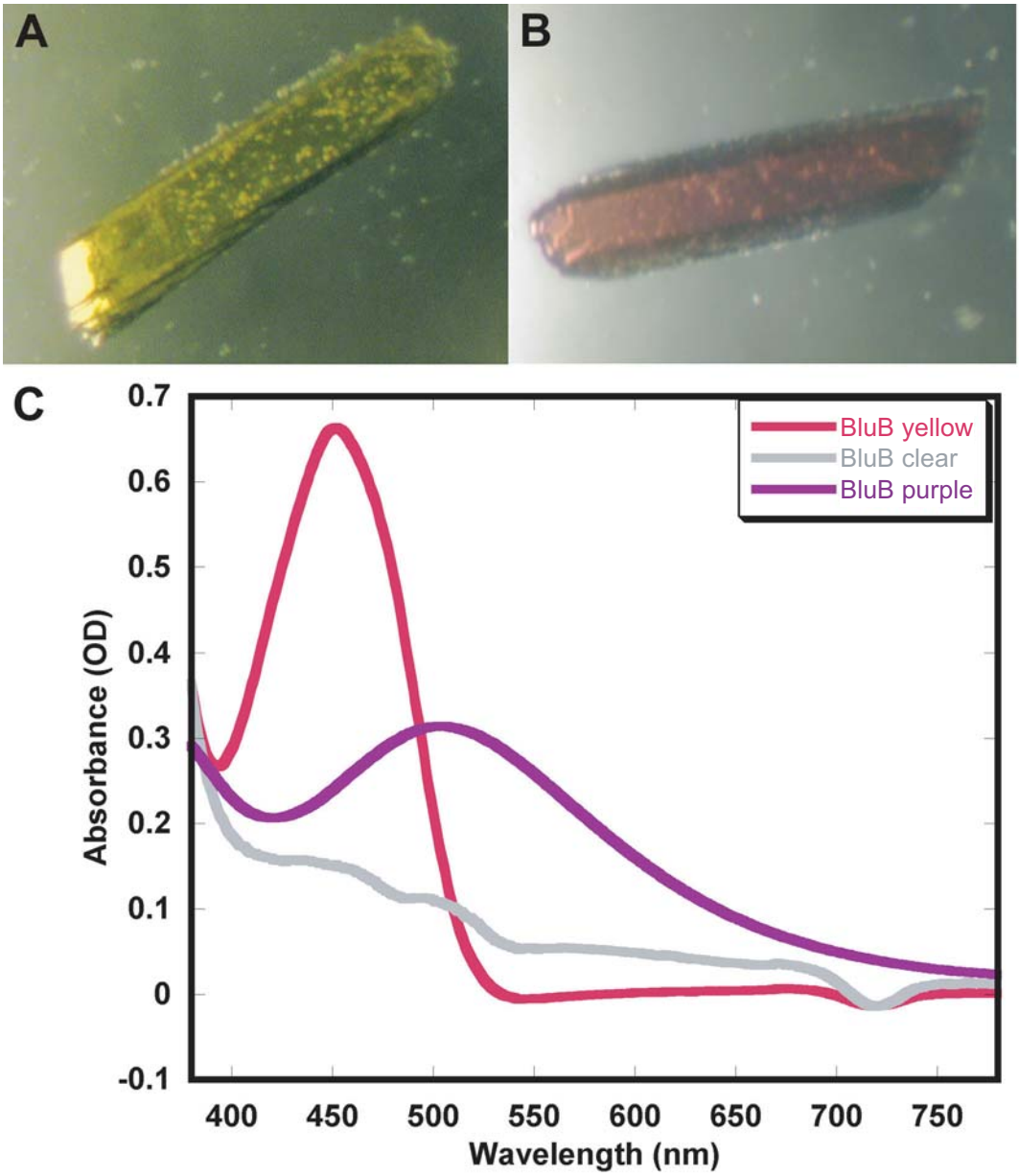

Supplementary Figure 7. Color change of BluB-FMN in the presence of dithionite. A. BluB-FMN crystals are pseudo-orthorhombic rods and bright yellow, due to the presence of FMN. **B.** BluB-FMN crystals soaked in saturated dithionite turn purple. **C.** Absorbance spectra of BluB. The spectra were measured at protein concentrations of 1 mg ml^{-1} (~40 M). The yellow BluB-FMN has a maximum absorbance at 452 nm (red spectrum). Under ambient oxygen, the yellow BluB-FMN becomes either (1) clear in 5 mM dithionite, due to reduction of FMN (gray spectrum), or (2) purple in ~15 mM dithionite (purple spectrum). The purple species likely represents an anionic charge transfer complex, and has a maximum absorbance at 504 nm. The purple species was not seen in the absence of BluB (not shown). Dithionite has a high background absorbance below 380 nm.

Supplementary Table 3. H-bonding distances in BluB-FMN and BluB-$FMNH_2$ structures

BluB-FMN[a]

	N5	O4		O2		N1	O2'	O4'		N1	C1'
1) Ser167 Oγ	3.30	3.57	1) Arg34 Nε	2.7	1) Arg34 NH2	2.9	2.8	4.1	1) Asp32 Oδ	3.5	3.4
2) Ser167 Oγ	2.97	3.26	2) Arg34 Nε	2.6	2) Arg34 NH2	3.1	3.0	3.7	2) Asp32 Oδ	3.5	3.5
3) Ser167 Oγ	3.09	3.42	3) Arg34 Nε	2.8	3) Arg34 NH2	3.4	3.2	3.8	3) Asp32 Oδ	3.4	3.3
4) Ser167 Oγ	3.05	3.38	4) Arg34 Nε	2.8	4) Arg34 NH2	3.2	2.9	3.7	4) Asp32 Oδ	3.6	3.5
5) Ser167 Oγ	2.81	3.02	5) Arg34 Nε	2.6	5) Arg34 NH2	3.1	3.1	4.1	5) Asp32 Oδ	3.4	3.3
6) Ser167 Oγ	3.07	3.52	6) Arg34 Nε	2.7	6) Arg34 NH2	3.2	3.1	4.0	6) Asp32 Oδ	3.3	3.4
7) Ser167 Oγ	2.99	3.24	7) Arg34 Nε	2.8	7) Arg34 NH2	3.4	3.3	3.8	7) Asp32 Oδ	3.3	3.4
8) Ser167 Oγ	2.94	3.49	8) Arg34 Nε	2.7	8) Arg34 NH2	3.4	3.4	3.9	8) Asp32 Oδ	3.3	3.1
average	**3.03**	**3.36**		**2.7**		**3.2**	**3.1**	**3.9**		**3.4**	**3.4**

BluB-$FMNH_2$[a]

	N5	O4		O2		N1	O2'	O4'		N1	C1'
1) Ser167 Oγ	3.22	3.36	1) Arg34 Nε	2.7	1) Arg34 NH2	3.1	3.0	3.8	1) Asp32 Oδ	3.1	3.7
2) Ser167 Oγ	3.02	2.91	2) Arg34 Nε	3.0	2) Arg34 NH2	3.2	2.6	3.0	2) Asp32 Oδ	3.4	3.1
3) Ser167 Oγ	3.12	3.18	3) Arg34 Nε	2.5	3) Arg34 NH2	2.9	2.7	3.9	3) Asp32 Oδ	2.9	3.5
4) Ser167 Oγ	3.01	2.87	4) Arg34 Nε	3.2	4) Arg34 NH2	3.3	2.6	3.1	4) Asp32 Oδ	3.5	3.4
5) Ser167 Oγ	3.31	3.85	5) Arg34 Nε	3.3	5) Arg34 NH2	4.2	2.8	3.3	5) Asp32 Oδ	3.1	2.5
6) Ser167 Oγ	3.14	3.21	6) Arg34 Nε	2.8	6) Arg34 NH2	4.3	3.5	4.2	6) Asp32 Oδ	2.7	2.5
7) Ser167 Oγ	3.00	3.38	7) Arg34 Nε	3.1	7) Arg34 NH2	3.7	2.8	4.0	7) Asp32 Oδ	3.0	3.4
8) Ser167 Oγ			8) Arg34 Nε	2.7	8) Arg34 NH2	3.4	3.2	4.2	8) Asp32 Oδ	3.5	2.9
average	**3.12**	**3.25**		**2.9**		**3.5**	**2.9**	**3.7**		**3.2**	**3.1**

[a] Crystals have eight subunits in each asymmetric unit. H-bonding distances between side chain atoms and flavin were measured for each subunit 1-8 and the average computed. The reduced crystal form that was re-oxygenated shows the most variability in H-bonding distances.

Supplementary Table 4. Crystallography data and refinement statistics

	PIP λ1	PIP λ2	PIP λ3	PIP λ4	BluB-FMN	BluB-CT	BluB-$FMNH_2$
Wavelength	1.0722	1.0725	1.0781	1.0332	0.9919	0.9919	0.9919
Resolution[a]	2.28	2.30	2.30	2.20	2.30	2.10	2.90
	2.37-2.28	2.38-2.30	2.38-2.30	2.28-2.20	2.38-2.30	2.18-2.10	3.00-2.90
Space Group	$P2_12_12_1$	$P2_12_12_1$	$P2_12_12_1$	$P2_12_12_1$	$P2_1$	$P2_1$	$P2_1$
Unique obs.	86284	85274	85948	94809	81156	94174	44966
Redundancy[a]	2.5 (1.9)	2.5 (2.0)	2.5 (2.0)	2.5 (1.8)	2.8 (2.7)	2.9 (2.7)	3.8 (3.7)
Completeness[a]	89.6 (71.0)	95.6 (92.0)	96.5 (82.1)	93.2 (61.7)	90.2 (91.8)	84.6 (82.9)	100.0 (100.0)
R_{sym}[a,b]	5.4 (22.9)	5.2 (23.3)	5.1 (22.3)	5.2 (25.1)	6.9 (19.4)	8.4 (21.2)	7.9 (31.5)
I / σ[a]	12.7 (1.9)	15.9 (2.3)	16.7 (2.5)	15.0 (1.9)	10.7 (3.3)	10.9 (3.1)	15.1 (3.3)

	BluB-FMN	BluB-CT	BluB-$FMNH_2$
Refined residues	1744	1744	1744
Refined waters	519	951	71
R_{cryst}[c]	20.7	20.4	21.7
R_{free}[d]	25.2	25.0	28.5
Average B-values ($Å^2$)			
BluB	21.5	20.2	36.6
FMN	15.2	18.9	35.2
Oxygen/Water[e]	23.9/13.5	21.8/12.7	22.7/8.0
Waters (all)	20.2	28.0	23.0
Ramachandran Statistics (%)			
Most favored	92.2	93.9	84.2
Additionally allowed	7.3	5.6	13.9
Generously allowed	0	0	1.0
Disallowed	0.5	0.5	0.8

MAD data used to determine the structure were collected from a BluB-FMN PIP derivative. Single wavelength data were collected for the yellow oxidized BluB-FMN, purple reduced charge transfer BluB-CT, and pale yellow/clear reduced BluB-$FMNH_2$

[a] Numbers in parenthesis refer to the highest resolution shell.

[b] $R_{sym} = [\Sigma_h\Sigma_i | I_i(h) - \langle I(h) \rangle | / \Sigma_h\Sigma_I I_i(h)] \times 100$, where $\langle I(h) \rangle$ is the average intensity of i symmetry related observations of reflections with Bragg index h.

[c] $R_{cryst} = [\Sigma_{hkl} |F_o - F_c| / \Sigma_{hkl} |F_o|] \times 100$, where F_o and F_c are the observed and calculated structure factors.

[d] R_{free} was calculated as for R_{cryst}, but on 5% of data excluded before refinement.

[e] Average B factor of oxygen or water when modeled into peak over the re-face of flavin.

SUPPLEMENTARY DISCUSSION

Although a definitive mechanism for BluB-mediated DMB formation from $FMNH_2$ is not possible at this point, Supplementary Scheme 1 outlines two possible mechanisms that would account for the BluB-catalyzed transformation of $FMNH_2$ to DMB, taking into consideration the experimental results obtained in this study. The formation of a flavin-4a-peroxy moiety (**5**) is highly likely, in parallel with the mechanism of flavin monooxygenases, a feature further supported by the presence of oxygen poised for reaction with $FMNH_2$ in the BluB active site (Fig. 3d). Moreover, the Asp32 and Ser167 mutants show signs of hydrogen peroxide generation, indicative of futile cycling of a flavin-peroxy species (Fig. 4). Whilst such a flavin-peroxy species is the canonical intermediate in flavin monooxygenase pathways[1], BluB is unique in its ability to harness its oxidative power for the destruction of bound FMN itself. We suggest that this is due to two unique features of the BluB active site: the complete isolation of FMN, and the unusual conformation of the FMN molecule bringing the ribityl chain into close proximity with the putative flavin-peroxy moiety.

Due to the challenging nature of this transformation, the overall pathway must contain some unusual steps. A unique intramolecular hydroxylation may be required to activate C1' for subsequent destruction of the flavin core (Supplementary Scheme 1a). The C1' hydroxylation that we propose is the single most challenging step in the reaction, requiring not only a difficult chemical transformation but also a major conformational change in BluB. This step would be facilitated by deprotonation at C1' by the critical catalytic residue Asp32. Direct intramolecular attack on the C4a-peroxy group would involve considerable strain on the flavin molecule. Equilibration via a cyclic endoperoxide to a flavin-C10a-peroxy species (not shown) would bring the reactive moiety into closer proximity with C1', though such an intermediate has not been

previously observed. We also recognize that the acidity of the C1' protons is low, so this mechanism would require an unusual active site micro-environment to drastically increase the basicity of Asp32.

Following this unusual step, however, hydroxylation at C1' would act as the key trigger for double fragmentation of the flavin core. A striking symmetry of reactivity is established across the molecule (**6**), with two carbinolamine groups dictating the subsequent destruction of FMN. The bond cleavage leading to intermediate **7** is set up by the carbinolamine of the 4a-hydroxy species **6**, and is mediated by Ser167. The new carbonyl of the ring-opened product may stabilize the otherwise unfavorable tautomer **8**, in turn acting as the electron-sink for a retro-aldol reaction. This retro-aldol involves the second carbinolamine (between N10 and C1') of intermediate **6** and generates E4P and the N-formyl species **10**, which would be readily transformed into DMB **3**.

The crystal structure of the ternary BluB-$FMNH_2$-O_2 complex (Fig. 3d) shows a direct interaction between dioxygen and the C2' hydroxyl group. Were this interaction to persist in the flavin-4a-peroxy intermediate **5**, one could imagine an alternative route for the oxidative cleavage involving abstraction of hydride from this position to cleave the C1'-C2' bond of the ribityl chain (Supplementary Scheme 1b). We are not aware of any biosynthetic precedent for such a transformation, however no other oxygen-dependent flavin enzymes are known in which the ribityl chain hovers over the flavin oxygen-binding site in such a conformation as observed for BluB (Fig. 3). Chemically, the peroxy group is susceptible to reduction by hydride ions[2], though hydride abstraction from the electrophilic oxygen of a hydroxyl group would be quite unusual. Following this highly unusual cleavage, the remainder of the transformation into DMB would be facile, again utilizing Ser167 to direct fragmentation of the carbinolamine of the flavin-4a-hydroxy

moiety. In such a scheme, we suggest that Asp32 plays a role in stabilizing the positive charge at C1' in intermediate **15** and/or in the transition state leading to its formation.

One particularly intriguing feature of these mechanistic proposals is the cleavage of the C4a-N5 carbinolamine of **6** or **15**. In all other known examples, water is lost from the flavin-hydroxy species, regenerating oxidized FMN; this route is facilitated by deprotonation at N5. We propose that, instead, BluB interacts with the oxygen of the 4a-hydroxy group to open the flavin B ring and thus drive the formation of DMB. Ser167 is a conserved residue amongst BluB homologues but is not found in related members of the nitroreductase/flavin oxidoreductase superfamily, where the hydrogen bond donor requirement is met by a backbone amide. Moreover, mutation of Ser167 to Gly or Cys drastically reduces the activity of BluB. This residue thus plays a key role in directing FMN fragmentation. Although the hydroxyl of Ser167 forms a hydrogen bond with N5 in our structures of BluB-FMN and BluB-$FMNH_2$ (Fig. 3a, b), only a subtle rotation about the Cα-Cβ bond would be required to bring it into close contact with the transient FMN-hydroxy group of **6** or **15**.

Previous studies have demonstrated the non-enzymatic conversion of (oxidized) FMN to DMB under basic conditions[3], suggesting a third possible route for this reaction. This non-enzymatic process was shown to proceed by initial base-catalyzed hydrolysis of the isoalloxazine ring, followed by oxidative cleavage to furnish DMB. It is possible that BluB catalysis follows an analogous route, however the necessity for (reduced) $FMNH_2$ and dioxygen in the BluB-mediated reaction suggest an alternative pathway proceeding through a peroxy-flavin moiety.

Further studies examining finer mechanistic aspects and the identities of transient and, as yet, cryptic intermediates are required to confirm the mechanistic details of this

transformation and to distinguish among these three (and other) possible routes. Nonetheless, it is apparent that this unique transformation requires some unusual individual steps, attesting to the chemical challenges facing BluB as it performs its catalytic cycle.

1. Tu, S. C. Reduced flavin: donor and acceptor enzymes and mechanisms of channeling. Antioxid Redox Signal. 3, 881-97. (2001).

2. Jin, H.-X., Liu, H.-H., Zhang, Q. & Wu, Y. On the susceptibility of organic peroxy bonds to hydride reduction. *J. Org. Chem.* **70**, 4240-4247 (2005).

3. Maggio-Hall, L. A., Dorrestein, P. C., Escalante-Semerena, J. C. & Begley, T. P. Formation of the dimethylbenzimidazole ligand of coenzyme B(12) under physiological conditions by a facile oxidative cascade. *Org. Lett.* **5**, 2211-3 (2003).

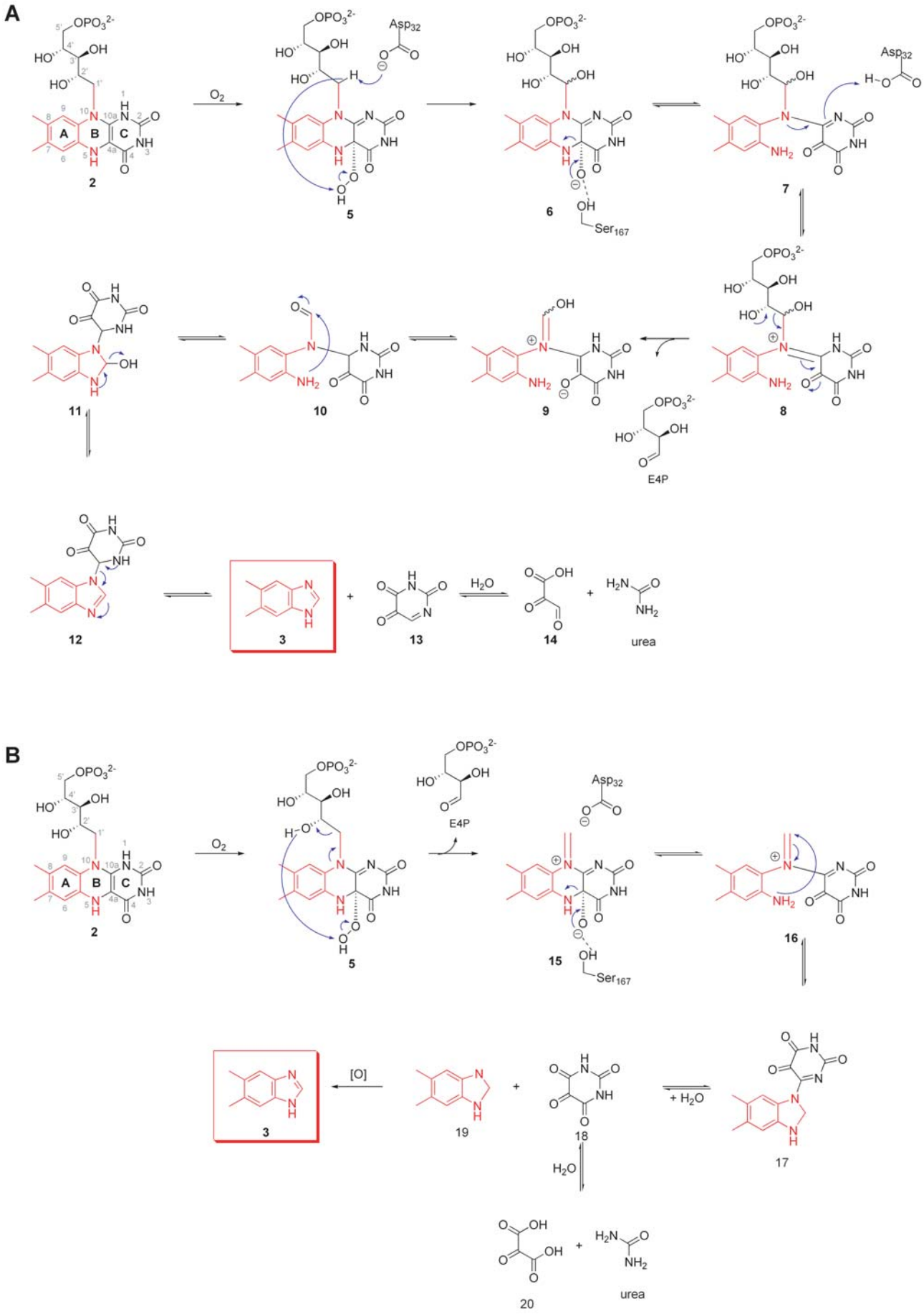

Supplementary Scheme 1

SUPPLEMENTARY METHODS

Expression and purification. BluB was cloned into pET28b (Novagen) via *Nde*I and *Xho*I restriction sites in frame with the vector encoded His tag and thrombin cleavage site. The enzyme was expressed in *E. coli*, purified by Ni-NTA chromatography, loaded with excess FMN, and digested overnight at 4 °C with 2 U thrombin mg^{-1} of BluB. The digest was stopped with 0.1 mM phenylmethylsulphonylfluoride and loaded onto an S200 sizing column equilibrated in 10 mM Tris pH 8.0, 10 mM NaCl, and 10 mM 2-mercaptoethanol. Peak fractions were pooled and concentrated to 36 mg ml^{-1} for biochemical characterization and crystallization. Mutant BluB expression constructs were made using the QuikChange site-directed mutagenesis kit (Stratagene).

Crystallization, structure determination, and refinement. Optimized BluB-FMN crystals grew in approximately one week from 0.7-1.1 M Ammonium Sulfate and 100 mM citrate pH 5.6. Crystals were frozen after immersion in a 20% (v/v) ethylene glycol substituted cryo-protectant. Heavy atom derivatives were obtained by soaking crystals for several hours in 10 mM di-μ-iodobis(ethylenediamine) diplatinum (PIP) and $LiSO_4$ substituted mother liquor, and then back soaking in PIP-free cryo-protectant. BluB-$FMNH_2$ crystals were obtained by soaking in excess dithionite followed by oxygen containing buffer. MAD data were collected from the PIP derivative, and single wavelength data were collected for oxidized and reduced BluB-FMN at the Advanced Light Source (ALS) beam-line 8.2.2 (Supplementary Table 4). The data were processed using HKL2000[1]. BluB crystals are pseudo-orthorhombic, belonging to space group $P2_1$ with a = 65 Å, b = 173 Å, c = 92 Å, β = 90.1° and four dimers per asymmetric unit. Heavy atom sites were obtained using SOLVE[2] and subsequently Arp/Warp[2] successfully traced one complete monomer and fragments of the others. This complete monomer was used as a molecular replacement model to find the remaining monomers using MOPREP[3]. Clear electron density was visible for FMN in both the oxidized and reduced crystals. The structures were refined with CNS[4] (Supplementary Table 4). Non-crystallographic symmetry (NCS) restraints were used during refinement of BluB-$FMNH_2$.

Production of [^{32}P]FMN

[^{32}P]FMN was produced by incubation of 200 μM riboflavin with 200 μM [γ-^{32}P]ATP, 5 mM $MgCl_2$, 10 mM HEPES pH 7.5, and 1 μM purified human riboflavin kinase[5]. Reactions were quenched after 20 h by heating to 100 ºC for 10 min. Conversion of riboflavin to FMN was confirmed by monitoring an identical reaction containing cold ATP by HPLC.

References

1. Otwinowski, Z. & Minor, W. Processing of x-ray diffraction data collected in oscilliation mode. *Methods Enzymol.* 276, 307-326. (1997).
2. Terwilliger, T. C. & Berendzen, J. Bayesian MAD phasing. *Acta Crystallogr*. D53, 571-579. (1997).
3. Vagin, A. & Teplyakov, A. MOLREP: an automated program for molecular replacement. *J. Appl. Cryst.*, 1022-1025. (1997).
4. Brünger, A. T. et al. Crystallography & NMR System: A new software suite for molecular structure determination. *Acta Crystallogr.* D54, 905-921. (1998).
5. Karthikeyan, S. et al. Crystal structure of human riboflavin kinase reveals a beta barrel fold and a novel active site arch. *Structure.* 11, 265-73. (2003).